Extraction of Material Parameters for Metamaterials Using a Full-Wave Simulator

Ahmad B. Numan and Mohammad S. Sharawi

Electrical Engineering Department
King Fahd University of Petroleum and Minerals (KFUPM)
Dhahran 31261, Saudi Arabia
Tel: + (966) 13860-4810; Fax: + (966) 13860-3535
E-mail: numan252@yahoo.com; msharawi@kfupm.edu.sa

Abstract

In this paper, a step-by-step procedure is devised for extracting the material parameters to facilitate and simplify the design procedure of metamaterial structures using commercial software packages. A parameter-retrieval method using the *S* parameters is used to calculate the curves for the complex permittivity and permeability of the metamaterial based on its unit element. The *S* parameters are extracted using *HFSS*™, which is a Finite-Element-Method (FEM)-based full-wave simulator. The permittivity and permeability curves are calculated using a *MATLAB* script. Two different methods are used in *HFSS* to extract the *S* parameters: one using perfect electric and perfect magnetic (PE-PM) boundary conditions, and the second using the master-slave boundary conditions. Wave ports and Floquet ports are used to excite the structure. The results of the proposed procedure are validated by comparing the calculated curves with already published results.

Keywords: Metamaterials; parameter extraction; electromagnetic modeling; electromagnetic fields

1. Introduction

Metamaterials are composite materials the electromagnetic properties of which not only depend on their material composition, but also on the inclusion of macroscopic structures that are specially designed to obtain a specific response. The properties of a material can hence be modified by introducing different structures within it. This behavior of metamaterials has made them very desirable for applications in a wide variety of frequency ranges, ranging from microwaves to optics.

Metamaterials are widely used in microwave devices to improve their performance. They are used in amplifiers [1, 2], filters [3-7], and power dividers [8-11]. In addition to microwave circuits, metamaterials are widely used in the design of antennas, as well. Since they can provide bandgaps, they are used to enhance the isolation between closely packed MIMO antenna systems [12, 13]. They are also used in antenna miniaturization [14-16] and to modify the characteristics of antennas [17, 18].

Metamaterials are usually realized by repeating a basic building block in a specific pattern. The basic building block is known as the unit element (UE), and it defines the basic properties of the metamaterial. In a simulator, metamaterials are modeled and simulated by introducing periodic boundary conditions applied on the boundaries of the unit element; it is assumed that the metamaterial is formed by an infinite array of the unit element in the direction of the periodic boundary conditions.

The selection and design of a metamaterial depends on the application and available resources. Metamaterials can be accurately designed using full-wave analysis, but it is a time-consuming task. On the other hand, a priori knowledge of the electromagnetic properties of the material will accelerate the design procedure. The electromagnetic properties, such as the complex permeability (μ) and the permittivity (ε) can be evaluated either by the analytical Drude-Lorentz model [19] or by the *S*-parameter-retrieval method [20-25]. The Drude-Lorentz method is not accurate, especially if the unit element of the metamaterial is a complex structure. On the other hand, the *S*-parameter-retrieval method depends on the *S* parameters extracted from the actual structure, and hence provides more-accurate values for the permittivity and permeability. In this work, we will rely on this method. The *S* parameters will be extracted from *HFSS*, which is a reliable and commercially available Finite-Element-Method (FEM)-based full-wave simulator. It is important to mention that this paper does not address the effectiveness of the *S*-parameter method in extracting the effective material parameters. Rather, it is a tutorial that devises a procedure for extracting these parameters to facilitate the design of the metamaterials. A detailed presentation of the S-parameter method and its ambiguities were given in [23].

Although the *S*-parameter-based method is well known, some detailed explanation is needed related to its application within a full-wave simulator having a metamaterial unit element, and the execution of the derived formulas to get the material parameters. This paper presents a tutorial that will discuss a complete procedure, showing the steps required to extract the material parameters for a metamaterial structure using a commercial software tool. We will start from the extraction of the *S* parameters and model excitation within a widely used full-wave simulator (*HFSS*). We then will explain and apply the *S*-parameter method, and provide a *MATLAB* script that can be used to get the curves of the metamaterial's complex permittivity and permeability.

2. Mathematical Formulation

In electromagnetics, the permittivity, permeability, and conductivity define the material's characteristics. The extraction of these values for different frequencies defines the propagation profile of the material at that frequency. In the extraction method used in this work, the refractive index and impedance of the material are used to extract the permittivity and permeability of the material under test.

To extract these material parameters (ε and μ), consider the unit element of a metamaterial with lattice vectors in all three dimensions. Appropriate boundary conditions and excitations are assigned to the different surface of the three-dimensional unit element to simulate the periodic metamaterial and excitation of this metamaterial to extract the *S* parameters. Consider a normally incident plane wave on the metamaterial cube, as shown in Figure 1. The *S* parameters of this system can be written as [25]

$$S_{11} = \frac{R_{01}\left(1 - e^{i2nk_0 d}\right)}{1 - R_{01}^2 e^{i2nk_0 d}}, \tag{1}$$

$$S_{21} = \frac{\left(1 - R_{01}^2\right) e^{i2nk_0 d}}{1 - R_{01}^2 e^{i2nk_0 d}}. \tag{2}$$

Solving Equations (1) and (2) gives

$$z = \pm\sqrt{\frac{\left(1 + S_{11}\right)^2 - S_{21}^2}{\left(1 - S_{11}\right)^2 - S_{21}^2}}, \tag{3}$$

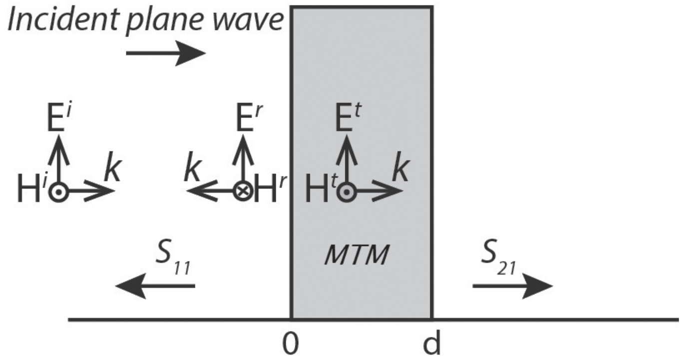

Figure 1. A normally incident plane wave on a metamaterial (MTM), placed in free space.

$$e^{ink_0 d} = \frac{S_{21}}{1 - S_{11}\dfrac{z-1}{z+1}}, \tag{4}$$

$$n = \frac{1}{k_0 d}\left[\left\{\left[\ln\left(e^{ink_0 d}\right)\right]'' + 2m\pi\right\} - i\left[\ln\left(e^{ink_0 d}\right)\right]'\right], \tag{5}$$

where $(\bullet)''$ represents the complex component and $(\bullet)'$ represents the real component of the complex number; S_{11} and S_{12} are reflection and transmission coefficients, respectively; R_{01} is $\frac{z-1}{z+1}$; n is the refractive index; z is the impedance; k_0 is the wavenumber; d is the maximum length of the unit element; m is the branch due to the periodicity of the sinusoidal function; E and H are electric and magnetic field components, respectively; and $(\bullet)^i$, $(\bullet)^r$, $(*)^r$ and $(\bullet)^t$ are the incident, reflected, and transmitted components of the fields, respectively.

In these expressions, the metamaterial is represented by the cube formed by the unit element, with appropriate boundary conditions and excitations. The material is assumed to be homogeneous, possessing an effective refractive index and impedance. This assumption is valid, as the dimensions of the unit element are usually less than one-tenth of the wavelength in the material.

The permittivity (ε) and permeability (μ) are related to the refractive index and impedance by the following expressions:

$$\varepsilon = \frac{n}{z}, \tag{6}$$

$$\mu = nz. \tag{7}$$

There are multiple solutions for the refractive index and the impedance, due to the multiple branches of the sinusoidal and the square-root functions. However, unique solutions can be reached by knowing the passive nature of the material, and avoiding the discontinuity in the resulting refractive index by appropriately selecting the branch (m in Equation (5)). In the case of the example selected for this tutorial, the largest dimension of the unit element is less than one-sixth of wavelength in the material at 10 GHz. This allows us to take the fundamental branch ($m = 0$) for a continuous refractive index [20, 23]. A detailed review of the *S*-parameter-extraction method and some clarifications were addressed in [23].

3. Extraction of the *S* Parameters

In order to extract the *S* parameters, a metamaterial is required to be realized. The realization of the metamaterial requires an infinite repetition of the unit element in the direction of the lattice vectors. This requirement is achieved by imposing boundary conditions on the unit element. There are two types of boundary conditions that are used to achieve the periodicity. The combination of perfect electric (PE) and perfect magnetic (PM) boundary conditions simulates the periodic boundary conditions by utilizing the symmetry inherited by the metamaterial due to the periodic repetition of the unit element [26]. In addition to perfect electric-perfect magnetic boundary conditions, *HFSS* provides master-slave boundary conditions to realize periodic boundary conditions. The boundary conditions at the master are enforced at the slave's surface, hence realizing an infinite periodic repetition.

The square-shaped split-ring resonator (SRR) structure, presented in [20], was selected to test the devised procedure. This reference was selected as it is one of the early and most accepted works in the literature for the extraction of material parameters using the *S* parameters. The split-ring resonator's layout is shown in Figure 2, and all the dimensions are in mm: $d\_out = 2.2$, $d\_in = 1.5$, $Wt = 0.2$, $S = 0.15$, $Gap = 0.3$, $L = 2.5$, $W = 0.14$, $a = b = c = 2.5$. The substrate used was FR-4, with a thickness of 0.25 mm and a dielectric constant of 4.4.

The periodic boundary conditions using perfect electric-perfect magnetic boundary conditions are shown in Figure 3, whereas the master-slave boundary conditions are shown in Figure 4. Although these two methods are equally effective in the case of a cubic-shaped unit element structure, the master-slave boundary conditions can cover complex polygon-shaped structures, as well. The boundary conditions can be set after selecting an appropriate side of the cube. After selecting the side, right click on the boundary and go to "Assign Boundary." Here, different boundary-condition options are listed. Select an appropriate boundary condition (Perfect E, Perfect H, Master, Slave). For Master or Slave boundary conditions, also specify the lattice vectors according to the design of the unit element. For Slave boundary condition, specify the name of its Master boundary. The lattice vectors (red and blue vectors on the plane) are shown in Figure 4.

Once the boundary conditions are set, the excitation ports are required to excite the structure. The excitation ports direct the incident wave to propagate from the top to bottom of the unit element, shown in Figure 2a. For excitation, *HFSS* provides two options. One option is to use the "Wave Port," while the other, which is more flexible, is to use the "Floquet port." A "Wave Port" is equivalent to a semi-infinite waveguide that can excite the structure with the incident wave perpendicular to the surface of the port. On the other hand, the "Floquet port" can simulate obliquely incident waves. This obliquely incident wave is important in situations where the direction of propagation of the incident wave is in the direction of periodicity. In this case, the "Wave Port" will not be able to excite the structure properties, as the plane perpendicular to the direction of propagation carries the periodic boundary conditions, and the "Wave Port" cannot be applied to these planes. The "Folquet Port" solves this problem by providing the obliquely incident excitation wave. In addition to this, the "Wave Port" does not provide any information about the propagation modes, whereas the "Floquet Port" provides the percentage of energy transferred

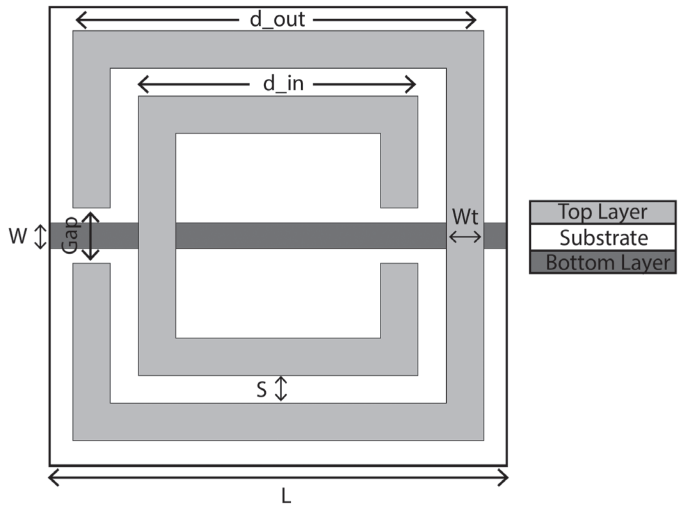

Figure 2a. The top view of the layout of a split-ring resonator (SRR).

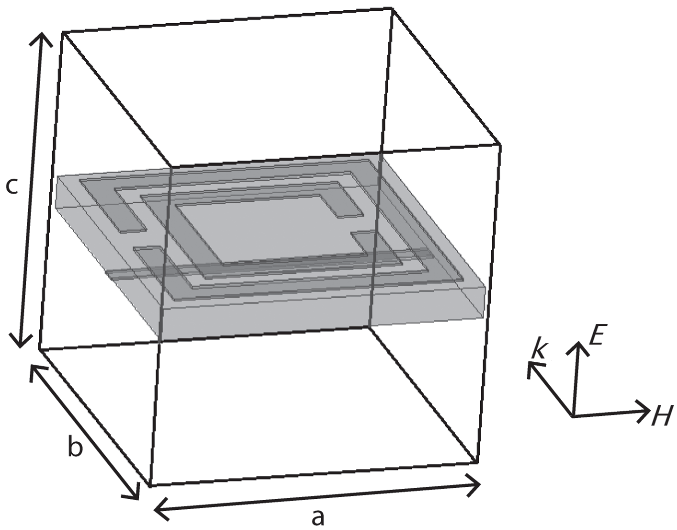

Figure 2b. The three-dimensional structure of the layout of a split-ring resonator (SRR).

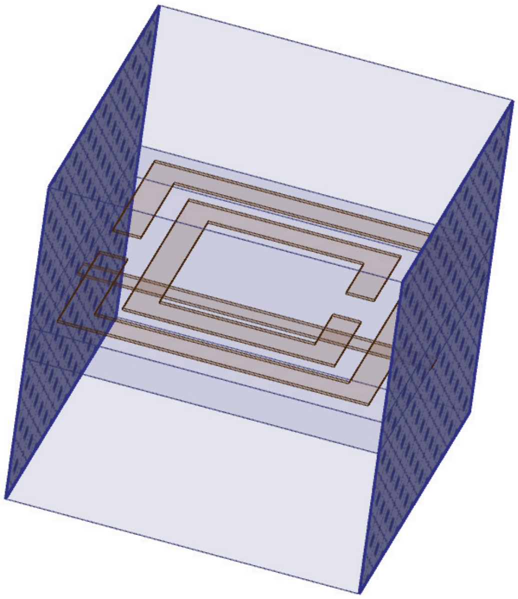

Figure 3a. The simulation model with perfect electric-perfect magnetic (PE-PM) boundary condition: perfect electric.

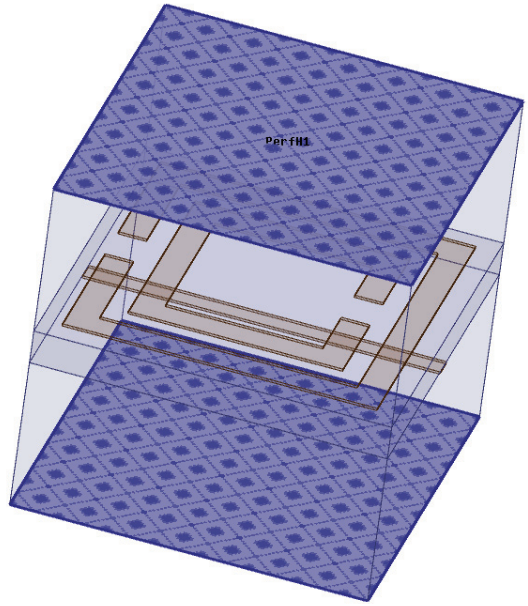

Figure 3b. The simulation model with the perfect electric-perfect magnetic (PE-PM) boundary condition: perfect magnetic.

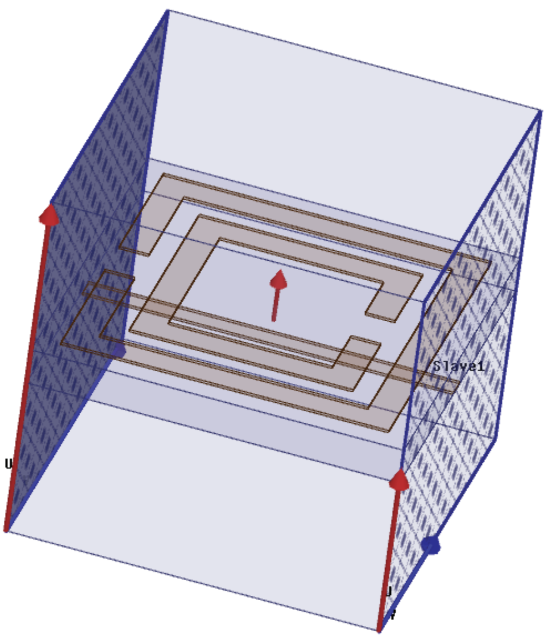

Figure 4a. The simulation model with the master-slave boundary condition: the first master-slave boundary pair.

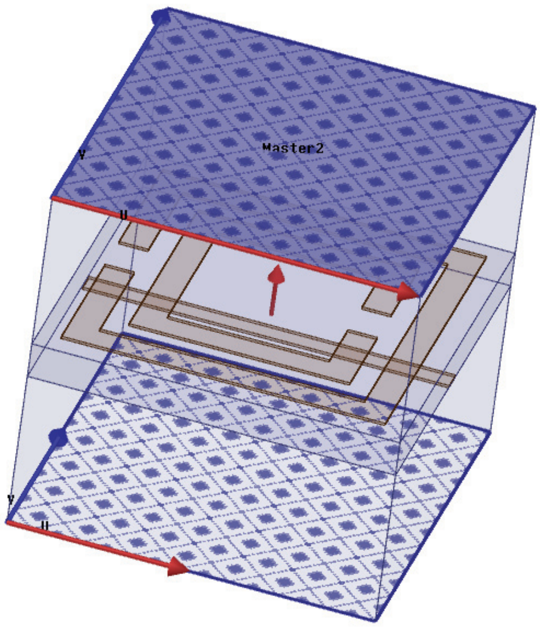

Figure 4b. The simulation model with the master-slave boundary condition: the second master-slave boundary pair.

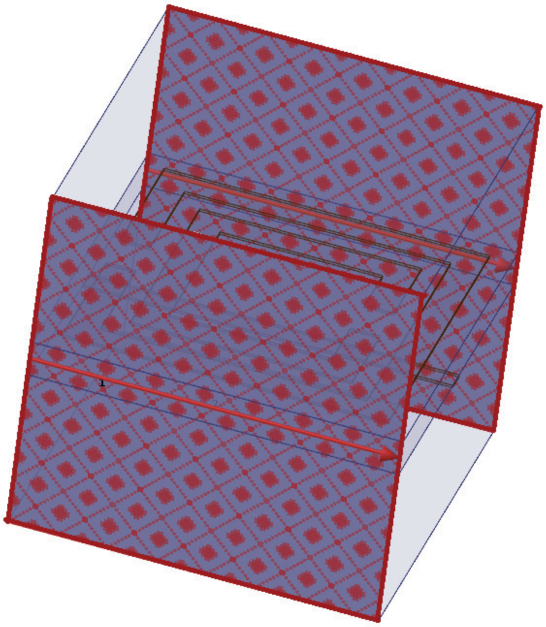

Figure 5a. The unit-element excitation: Wave Port.

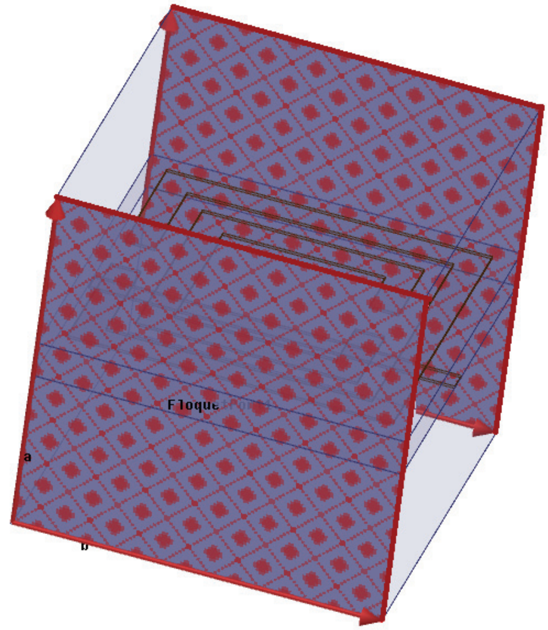

Figure 5b. The unit-element excitation: Floquet Port.

by a specific mode [27]. However, the "Floquet Port" can only be used with the master-slave boundary conditions. "Wave Port" and "Floquet Port" excitations are shown in Figures 5a and 5b, respectively.

Once the boundary conditions and excitations are properly assigned to the structure, you need to add the analysis setup. Set the appropriate solution frequency (10 GHz in this case), and simulate the structure. After the simulation is complete, extract the magnitude and phase of the *S* parameters. For "Floquet Port" excitation, the *S* parameters are extracted based on the dominant mode that is responsible for the majority of the power transfer [27]. The *S*-parameter curves of the structure modeled in Figure 2 are shown in Figures 6a and 6b for the magnitude and phase, respectively. In comparison with the *S*-parameter curves published in [20], it was clear that the results shown in Figure 6 were frequency reversed compared to the published results. This was due to the fact that the expressions derived for the permittivity and permeability were based on the formulation presented in [28], which assumed the time factor of $e^{j\omega t}$, whereas *HFSS* assumes this factor to be $e^{-j\omega t}$. Since the *S* parameters are in the frequency domain, the time-reversal property of the Fourier transform is applied to the *S* parameters according to

$$F\left[x(-t)\right] = X(-\omega). \tag{8}$$

The *S* parameters used to derive the material parameters are hence frequency reversed relative to the *S* parameters extracted from the simulator.

4. Obtaining the Material Parameter Curves from the Extracted *S* Parameters

Once the *S* parameters are extracted and verified from the published results, the parameters are derived using a *MATLAB* script, which uses the expressions presented in the mathematical formulation to derive the complex permittivity and permeability curves [25]. The *MATLAB* script requires the *S* parameters as input files. The input files are in comma separated values (`csv`) format. When the *S* parameters are saved/extracted from the *HFSS* simulations, they can be saved in `csv` format. These files contain three columns, where the first column lists the frequency, the second column contains the magnitude, and the last column contains the phase information. According to the script, two different files are required: one for $S11$ and the other for $S21$. Since these *S* parameters are extracted from *HFSS*, they are reversed to make them compatible with the formulation, according to Equation (8). Finally, the derived expressions are used to calculate the curves for the permittivity and the permeability.

Figure 7 shows the *MATLAB* script used to calculate the metamaterial-parameter curves based on the extracted *S* parameters, while Figure 8 shows the function used in Figure 7 to read the data from the data files extracted from *HFSS* in `csv` format (other formats, such as `txt` format, can be extracted from *HFSS*, and the user has to use an appropriate function to open such files). Both files have comments to make the commands and their effects easy to understand.

The permittivity and permeability curves obtained are shown in Figures 9a and 9b. They closely matched the curves already published in [20] for the split-ring-resonator-wire metamaterial structure. These figures showed that the permit-

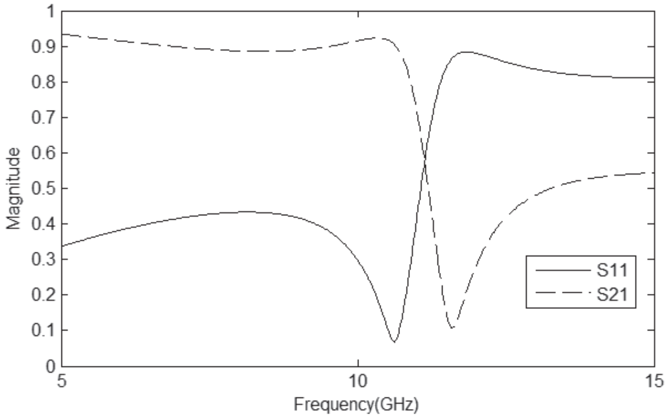

Figure 6a. The magnitude of the *S* parameters obtained from *HFSS*.

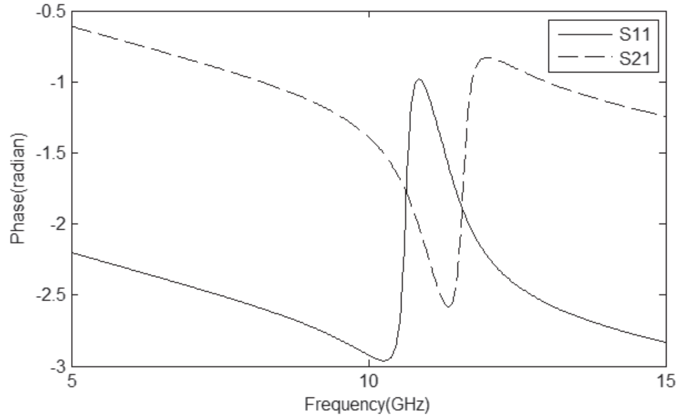

Figure 6b. The phase of the *S* parameters obtained from *HFSS*.

```
clc
clf
clear
S11=DATA_READ('C:\Users\Ahmed\Desktop\S11.csv');
S21=DATA_READ('C:\Users\Ahmed\Desktop\S21.csv');
S11(:,2:3)=flipud(S11(:,2:3));  % Frequency reversal
S21(:,2:3)=flipud(S21(:,2:3));  % Frequency reversal
s11=S11(:,2).*(cos(S11(:,3))+i*sin(S11(:,3)));%Complex S-parameters
s21=S21(:,2).*(cos(S21(:,3))+i*sin(S21(:,3)));%Complex S-parameters
f=S11(:,1)*1e9; %Frequency range
c=3e8;          %Speed of light
k=(2*pi/3e8)*f; %Wave Number
d=2.5e-3;       % Largest dimension of UE

z=((((1+s11).^2)-s21.^2)./(((1-s11).^2)-s21.^2)).^0.5;      % eq. 3
tmp=(z-1)./(z+1);
exp=s21./(1-s11.*tmp);                                 % eq. 4
n=(imag(log(exp))-i.*real(log(exp)))./(k*d);           % eq. 5


eps_eff= n./z; % eq. 6
mu_eff=  n.*z; % eq. 7
% Plot the curves
plot(S11(:,1),real(eps_eff),'--k',S11(:,1),real(mu_eff),'k')
legend('Re(\epsilon_e_f_f)','Re(\mu_e_f_f)')
xlabel('Frequency(GHz)');
ylabel('Real permittivity and permeability')
figure
plot(S11(:,1),imag(eps_eff),'--k',S11(:,1),imag(mu_eff),'k')
legend('Img(\epsilon_e_f_f)','Img(\mu_e_f_f)')
xlabel('Frequency(GHz)')
ylabel('Imaginary permittivity and permeability')
figure
plot(S11(:,1),real(n),'--k',S11(:,1),real(z),'k')
legend('Re(n)','Re(z)')
xlabel('Frequency(GHz)')
ylabel('Real refractive index and impedance')
figure
plot(S11(:,1),imag(n),'--k',S11(:,1),imag(z),'k')
legend('Img(n)','img(z)')
xlabel('Frequency(GHz)')
ylabel('Imaginary refractive index and impedance')
```

Figure 7. A *MATLAB* script for calculating the effective μ and ε curves.

```
fid = fopen(path,'rt');          %Open the file
fi = fopen('G:\temp.csv','w');%Open temporary file
tline = fgets(fid);                    %Read first line
while ~feof(fid)                 %Write numeric data in temporary file
tline = fgets(fid);
fprintf(fi,tline);
end
fclose(fid);
fclose(fi);
x=csvread('G:\temp.csv');        % Read temporary file data
delete('G:\temp.csv')            % Delete temporary file
```

Figure 8. The function to read data from the *HFSS* `csv` data file.

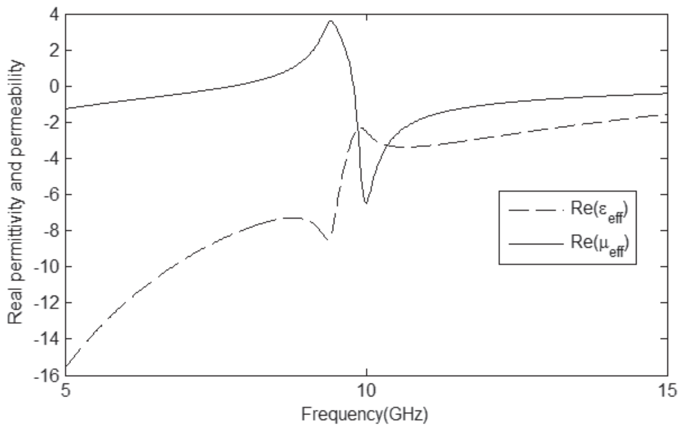

Figure 9a. The real values of permittivity and permeability.

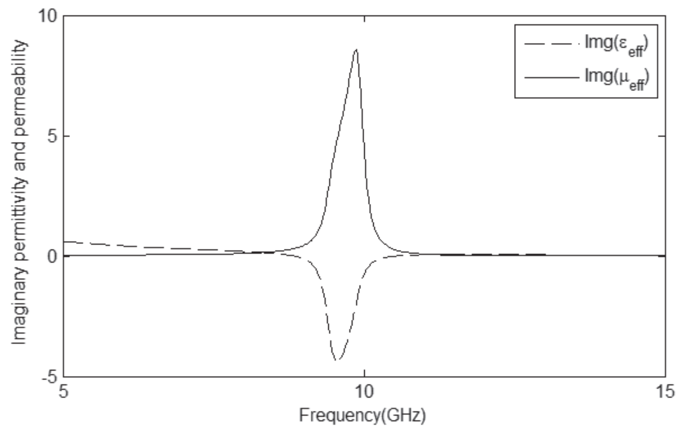

Figure 9b. The imaginary values of permittivity and permeability.

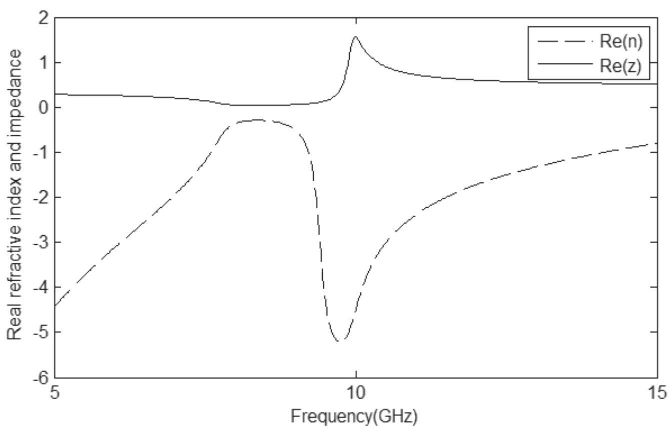

Figure 10a. The real curves for refractive index and impedance.

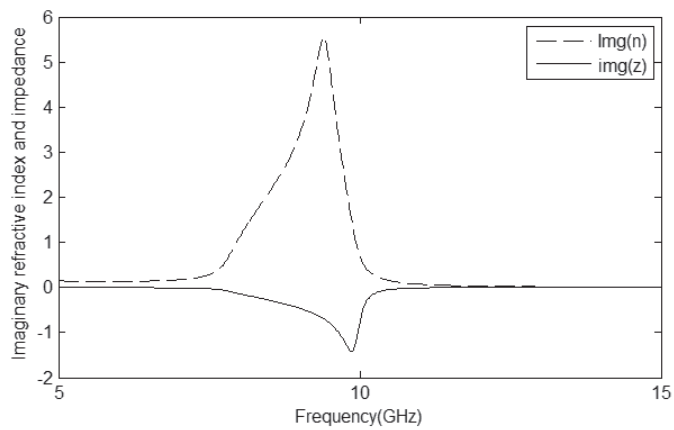

Figure 10b. The imaginary curves for refractive index and impedance.

- Run HFSS
- Save the project
- Insert new HFSS Design
  Project --> Insert HFSS Design
- Draw the substrate
  - Draw --> Box
  - Draw a random box in 3D Modeler window
  - In the 3D modeler tree, double click on under Solid--> Vacuum--> Box1
  - Change the "name" to subs and "color" and "transparent" properties according to your convenience
  - Change "material" to "FR-4 epoxy"
  - Click OK to close the dialog
  - Double click Solid--> FR4_epoxy--> subs -->CreateBox
  - Write "-1.25mm ,-1.25mm ,-0.125mm " in "position"
  - Write "2.5mm" in both "XSize" and "YSize"
  - In "ZSize", write 0.25mm
  - Click OK to close the dialog
- Draw the outer ring of the SRR
  - Draw a random box in 3D Modeler window
  - Set its material copper and name it as Outer_SRR1
  - Set the position as " -1.1mm ,-1.1mm ,0.125mm"
  - Set the XSize=2.2mm, YSize=2.2mm,ZSize=0.017
  - Draw another random box in 3D Modeler window
  - Set its material copper and name it as Outer_SRR2
  - Set the position as " -0.9mm ,-0.9mm ,0.125mm"
  - Set the XSize=1.8mm, YSize=1.8mm,ZSize=0.017
  - Draw another random box in 3D Modeler window
  - Set its material copper and name it as GAP1
  - Set the position as "-0.15mm ,-1.1mm ,0.125mm"
  - Set the XSize=0.3mm, YSize=0.2mm,ZSize=0.017
  - Now select both Outer_SRR1 and then Outer_SRR2(order is important, use "Ctrl" key to select both geometries)
  - Subtract the two geometries (Modeler--> Boolean --> Subtract) (press OK in opened dialog without making any change)
  - Select Outer_SRR1 and then GAP1 and subtract the two geometries. This will complete the design of outer ring of SRR
- Draw the inner ring of the SRR
  - Draw a random box in 3D Modeler window
  - Set its material copper and name it as Inner_SRR1
  - Set the position as " -0.75mm ,-0.75mm ,0.125mm"
  - Set the XSize=1.5mm, YSize=1.5mm,ZSize=0.017
  - Draw another random box in 3D Modeler window
  - Set its material copper and name it as Inner_SRR2
  - Set the position as " -0.55mm ,-0.55mm ,0.125mm"
  - Set the XSize=1.1mm, YSize=1.1mm,ZSize=0.017
  - Draw another random box in 3D Modeler window
  - Set its material copper and name it as GAP2
  - Set the position as "-0.15mm ,0.55mm ,0.125mm"
  - Set the XSize=0.3mm, YSize=0.2mm,ZSize=0.017
  - Now select Inner_SRR1 and then Inner_SRR2(order is important)
  - Subtract the two geometries (Modeler--> Boolean --> Subtract)
  - Select Inner_SRR1 and then GAP2 and subtract the two geometries. This will complete the design of inner ring of SRR Set its material copper and name it as GAP2
  - Set the position as "-0.15mm ,0.55mm ,0.125mm"
  - Set the XSize=0.3mm, YSize=0.2mm,ZSize=0.017
  - Now select Inner_SRR1 and then Inner_SRR2(order is important)
  - Subtract the two geometries (Modeler--> Boolean --> Subtract)
    Select Inner_SRR1 and then GAP2 and subtract the two geometries. This will complete the design of inner ring of SRR
- Draw a wire
  - Draw another random box in 3D Modeler window
  - Set its material copper and name it as Wire
  - Set the position as "-0.07mm ,-1.25mm ,-0.125mm"
  - Set the XSize=0.14mm, YSize=2.5mm,ZSize=-0.017mm
- Draw the UE box
  - Draw another random box in 3D Modeler window
  - Set its material air and name it as UE
  - Set the position as "-1.255mm ,-1.255mm ,-1.255mm "
  - Set the XSize=2.51mm, YSize=2.51mm,ZSize=2.51mm

Setting up the simulation

- Apply Boundary conditions
  - Right click on the UE face perpendicular to +x axis and select Assign Boundary --> Master
  - Define U-Vector as shown in Figure 4
  - Select and right click on the face of UE that is perpendicular to -x axis and select Assign Boundary --> Slave
  - Now select the UE face perpendicular to +y-axis and assign master boundary condition
  - Similarly select face perpendicular to -y-axis and assign the slave boundary condition
- Apply Excitations
  - Select and right click on face of UE perpendicular to +z axis
  - Select Assign Excitation --> Floquet Port. Technical details about Floquet port is given in [27]
  - Define "A Direction" and "B Direction" as shown in Figure 5(b) and click Next in Floquet Port setup dialog
  - Set Number of Modes as 2
  - Click on Modes Calculator and set frequency as 10GHz
  - Click on Next. This will open Post Processing tap. Do not change anything here
  - Click Next to 3D Refinement and Check Affects Refinement for both TE and TM Modes
  - Click OK to complete the setup
  - Similarly apply the Floquet port on face of UE perpendicular to -z axis
- Add Solution setup at 10GHz
- Add frequency Sweep form 1 to 20GHz with interpolating "sweep type"
- Run the simulation and get magnitude and phase of the s-parameters

Figure 11. A step-by-step procedure to obtain S parameters for the split-ring-resonator-wire unit element [19] using *HFSS*.

tivity was negative in the frequency range of 7.85 GHz to 9.4 GHz, and both the permittivity and permeability were negative in the frequency range of 8.8 GHz to 9.4 GHz, showing double-negative metamaterial characteristics. The refractive index and the impedance are shown in Figures 10a and 10b. These figures showed negative real refractive index and positive impedance, which showed the metamaterial behavior in the region of interest.

Figure 11 provides a step-by-step guide for creating a unit-element metamaterial structure and setting up the simulation to get the *S* parameters used in the presented material parameters extraction process. These steps are based on *HFSS version 13*. Some minor variations might be observed in other, higher versions of this tool. Once the code in Figure 11 is carried out, the code in Figures 7 and 8 should be used to plot the resultant material curves, as discussed earlier in this article.

5. Conclusions

In this work, a complete step-by-step procedure for obtaining the material parameters of a metamaterial structure was presented based on the *S* parameters extracted from a full-wave simulator (*HFSS*). The procedure was illustrated by calculating the permittivity and permeability curves for a split-ring resonator. The accuracy of the curves obtained was verified by comparing them to some published results. Two different types of periodic boundary conditions were presented. In addition to the periodic boundary conditions, two different types of excitations were also used and discussed in this work. The differences between them were highlighted. The procedure will help researchers in this area to extract metamaterial property curves with ease, using commercially available software.

6. Acknowledgements

The authors would like to thank the Associate Editor of the Education Column, Karl Warnick, as well as the reviewers, for their detailed comments and suggestions, which enhanced the content of the paper. The authors would also like to thank the Deanship of Scientific Research (DSR) at KFUPM for supporting parts of this work through project number RG1219.

7. References

1. H. Kim and C. Seo, "Inverse Class-F Power Amplifier Using the Metamaterial Structure on the Harmonic Control Circuit," *Microwave and Optical Technology Letters*, **50**, 11, February 2008, pp. 2881-2884.

2. C. Tseng and C. Chang, "Microwave Push-Pull Power Amplifier Using Metamaterial-Based Baluns," Asia-Pacific Microwave Conference (APMC), December 2008, pp.1-4.

3. S. Awasthi, A. Biswas and M. J. Akhtar, "Compact Bandstop Filter Using Triangular Metamaterial Mushroom Resonators," Asia-Pacific Microwave Conference Proceedings (APMC), December 2012, pp. 217-219.

4. Z. M. Thomas, T. M. Grzegorczyk, B. Wu and J. A. Kong, "Enhanced Microstrip Stopband Filter Using a Metamaterial Substrate," *Microwave and Optical Technology Letters*, **48**, 8, February 2006, pp. 1522-1525.

5. C. Lee, K. M. K. H. Leong and T. Itoh, "Metamaterial Transmission Line Based Bandstop and Bandpass Filter Designs Using Broadband Phase Cancellation," IEEE MTT-S International Microwave Symposium Digest, June 2006, pp. 935-938.

6. M. Morata, I. Gil and R. Fernandez-Garcia, "Parametric Design of Stop Band Pass Filter Based on RF Metamaterials in LTCC Technology," Progress in Electromagnetics Research Symposium Proceedings, August 2012, pp. 813-817.

7. I. A. I. Al-Naib, C. Jansen, and M. Koch, "Single Metal Layer CPW Metamaterial Bandpass Filter," *Progress in Electromagnetics Research Letters*, **17**, 2010, pp. 153-161.

8. C. Tseng and Chih-Lin Chang, "A Broadband Quadrature Power Splitter Using Metamaterial Transmission Line," *IEEE Microwave and Wireless Components Letters*, **18**, 1, January 2008, pp. 25-27.

9. M. A. Antoniades and G. V. Eleftheriades "A Broadband Series Power Divider Using Zero-Degree Metamaterial Phase-Shifting Lines," *IEEE Microwave and Wireless Components Letters*, **15**, 11, November 2005, pp. 808-810.

10. C. Tseng and C. Chang, "Improvement of Return Loss Bandwidth of Balanced Amplifier Using Metamaterial-Based Quadrature Power Splitters," *IEEE Microwave and Wireless Components Letters,* **18**, 4, April 2008, pp. 269-271.

11. K. W. Eccleston, "Planar N-way Metamaterial Power Divider," Asia Pacific Microwave Conference (APMC), December 2009, pp. 1024-1027.

12. M. S. Sharawi, A. B. Numan, and D. N. Aloi, "Isolation Improvement in a Dual-Band Dual-Element MIMO Antenna System Using Capacitively Loaded Loops," *Progress In Electromagnetics Research*, **134**, 2013, pp. 247-266.

13. K. Sarabandi and Y. J. Song, "Subwavelength Radio Repeater System Utilizing Miniaturized Antennas and Metamaterial Channel Isolator," *IEEE Transactions on Antennas and Propagation*, **59**, 7, July 2011, pp. 2683-2690.

14. R. O. Ouedraogo and E. J. Rothwell, "Metamaterial Inspired Patch Antenna Miniaturization Technique," IEEE Antennas and Propagation Society International Symposium, July 2010, pp. 1-4.

15. I. Singh, V. S. Tripathi, and S. Tiwari, "Dual-Band Microstrip Patch Antenna Miniaturization Using Metamaterial," *Journal of Engineering*, March 2013, pp. 1-5.

16. M. S. Sharawi, M. U. Khan, A. B. Numan and D. N. Aloi, "A CSRR Loaded MIMO Antenna System for ISM Band

Operation," *IEEE Transactions on Antennas and Propagation*, **AP-61**, 8, August 2013, pp. 4265-4274

17. D. B. Brito,A. G. d'Assuncao, R. H. C. Maniçoba, X. Begaud, "Metamaterial Inspired Fabry-Pérot Antenna with Cascaded Frequency Selective Surfaces," *Microwave and Optical Technology Letters*, **55**, 5, May 2013, pp. 981-985.

18. W. Cao, A. Liu, B. Zhang, T. Yu, Z. Qian, "Dual-Band Spiral Patch-Slot Antenna with Omnidirectional CP and Unidirectional CP Properties," *IEEE Transactions on Antennas and Propagation*, **AP-61**, 4, April 2013, pp. 2286-2289.

19. C. R. Simovski, Belov, A. P. Bavel and S. He, "Backward Wave Region and Negative Material Parameters of a Structure Formed by Lattices of Wires and Split-Ring Resonators," *IEEE Transactions on Antennas and Propagation*, **AP-51**, 10, October 2003, pp. 2582-2591.

20. D. R. Smith, D. C. Vier, Th. Koschny and C. M. Soukoulis, "Electromagnetic Parameter Retrieval from Inhomogeneous Metamaterials," *Physics Review E*, **71**, 3, 2005, 036617.

21. P. Markoš and C. M. Soukoulis, "Transmission Properties and Effective Electromagnetic Parameters of Double Negative Metamaterials," *Optics Express*, **11**, April 2003, pp. 649-661

22. R. W. Ziolkowski, "Design, Fabrication, and Testing of Double Negative Metamaterials," *IEEE Transactions on Antennas and Propagation*, **AP-51**, 7, July 2003, pp. 1516-1528.

23. S. Arslanagic, T. V. Hansen, N. A. Mortensen, A. H. Gregersen, O. Sigmund, R. W. Ziolkowski and O. Breinbjerg "A Review of the Scattering-Parameter Extraction Method with Clarification of Ambiguity Issues in Relation to Metamaterial Homogenization," *IEEE Antennas and Propagation Magazine*, **55,** 2, April 2013, pp. 91-106

24. D. R. Smith, S. Schultz, P. Markos, and C. M. Soukoulis, "Determination of Effective Permittivity and Permeability of Metamaterials from Reflection and Transmission Coefficients," *Physics Review B*, **65**, 19, April 2002, 195104.

25. X. Chen, T. M Grzegorcezyk, B. Wu, J. Pacheco, Jr., and J. A. Kong "Robust Method to Retrieve the Constitutive Effective Parameters of Metamaterials," *Physics Review E*, **70**, July 2004, 016608.

26. A. Andreone, A. Cusano, A. Cutolo, V. Galdi, *Selected Topics in Photonic Crystals and Metamaterials*, World Scientific Publishing Co. Pte. Ltd., 2011, pp. 202-205.

27. HFSS™, "Getting Started with HFSS: Floquet Ports," Technical Report, 2010.

28. B. William Weir, "Automatic Measurement of Complex Dielectric Constant and Permeability at Microwave Frequencies," *Proceedings of the IEEE*, **62**, 1, January 1974, pp. 33-36.

Introducing the Authors

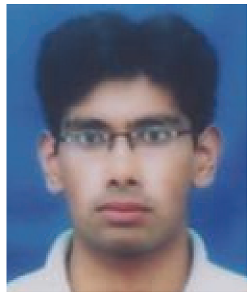

Ahmad B. Numan received his BSc from the University of Engineering and Technology, Lahore, Pakistan, in 2009. He worked as a research assistant at Al-Khawarizmi Institute of Computer Sciences (KICS)-UET, Lahore, until 2011. Currently, he is pursuing his MS in Electrical Engineering at King Fahd University of Petroleum and Minerals (KFUPM), Dhahran, Saudi Arabia. He is interested in applied electromagnetics, including antenna system design.

Mohammad S. Sharawi is an Associate Professor of Electrical Engineering at King Fahd University of Petroleum and Minerals (KFUPM), Dhahran, Saudi Arabia. He was born in Wolfsburg, Germany, in 1977. Dr. Sharawi is the founder and Director of the Antennas and Microwave Structure Design Laboratory (AMSDL). He was a Research Scientist with the Applied Electromagnetics and Wireless Laboratory in the Electrical and Computer Engineering Department, Oakland University, Michigan, USA, during 2008-2009. Dr. Sharawi was a faculty member in the Computer Engineering Department at Philadelphia University, Amman, Jordan, during 2007-2008. He served as the Organization Chair of the IEEE Conference on Systems, Signals and Devices that was held in Jordan in July 2008. He served on several IEEE conference technical committees, especially for the Antennas and Propagation Symposium (AP-S). He obtained his PhD in RF Systems Engineering from Oakland University, Michigan, USA, in 2006. During 2002-2003, he was a hardware design engineer with Silicon Graphics Inc., California, USA. Dr. Sharawi has more than 80 refereed international journal and conference paper publications. His research interests include printed and MIMO antenna design and characterization, RF electronics, applied electromagnetics, wireless communications and hardware integration. He has one issued, three published, and seven pending patents. Dr. Sharawi is a Senior Member of the IEEE.